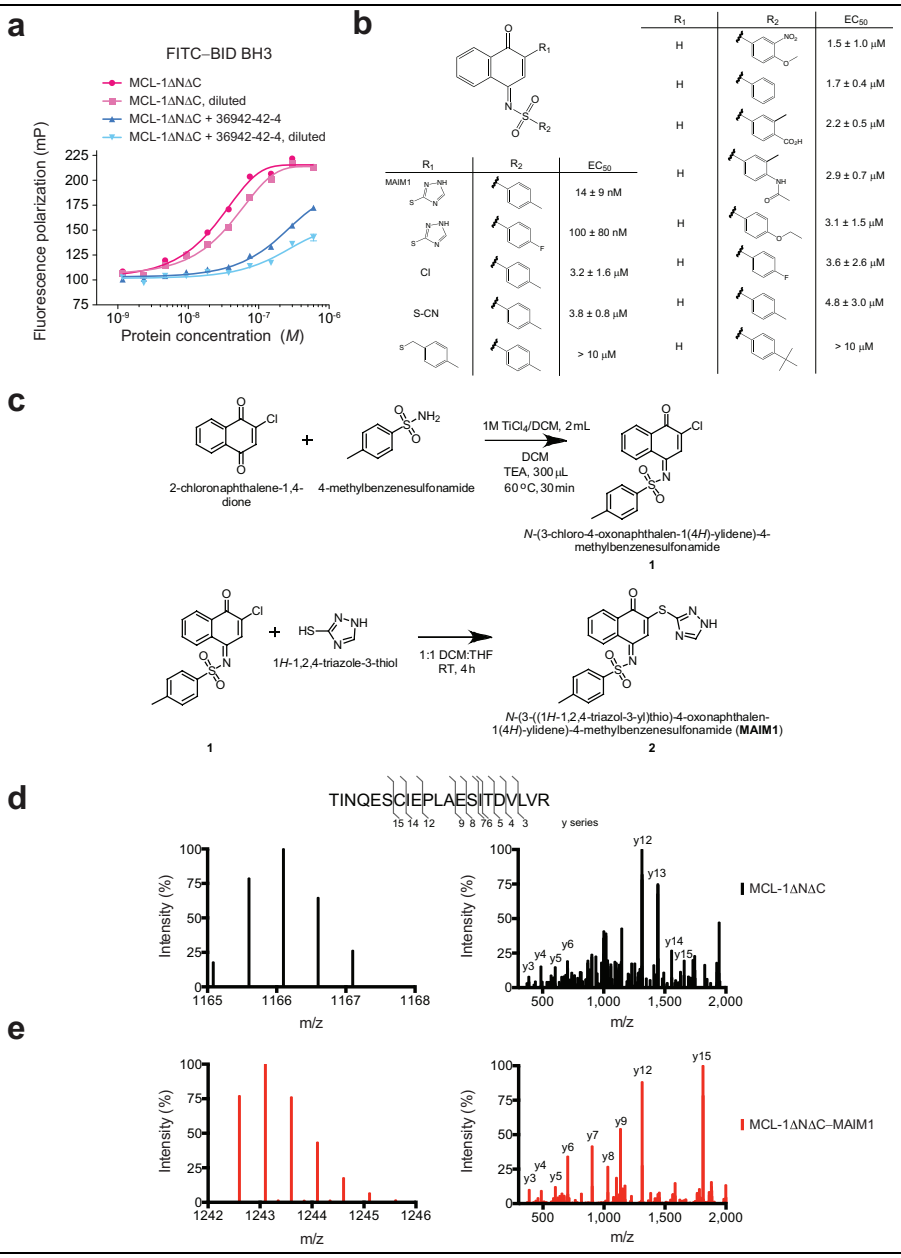

Supplementary Figure 1

Small molecule covalent inhibition of MCL-1ΔNΔC

(a) Fluorescence polarization dilutional binding assay of FITC–BID BH3 and MCL-1ΔNΔC in the presence and absence of N-(4-hydroxy-1-naphthalenyl)-benzenesulfonamide (CAS# 36942-42-4), a small molecule screening hit that exhibited irreversible inhibition of the BH3-binding activity of MCL-1ΔNΔC. **(b)** Chemical structures of MAIM1 analogs that emerged from our competitive MCL-1 SAHB$_A$–MCL-1ΔNΔC screen. Competitive potency corresponded to compound reactivity, based on the nature of the leaving group (R1) and electron withdrawing capacity (R2). Data are mean ± s.e.m. (n = 3 technical replicates). **(c)** Chemical synthesis of MAIM1. **(d-e)** Trypsin digestion and LC-MS/MS of unmodified **(d)** and MAIM1-conjugated **(e)** MCL-1ΔNΔC. Full scan spectra (left) demonstrate the peptide containing unmodified C286 (mass: 2329.18 Da) and the MAIM1 conjugate (mass: 2483.19 Da), reflecting the added mass of cleaved MAIM1 adduct (i.e. minus tosyl). MS/MS spectra (right) further confirm MAIM1 conjugation at position C286. Whereas the masses of ions y3, y4, y5, y6, and y12 are shared between the peptides, there is a discrete mass shift for ion y15, which contains C286. For clarity, only the y ions are labeled.

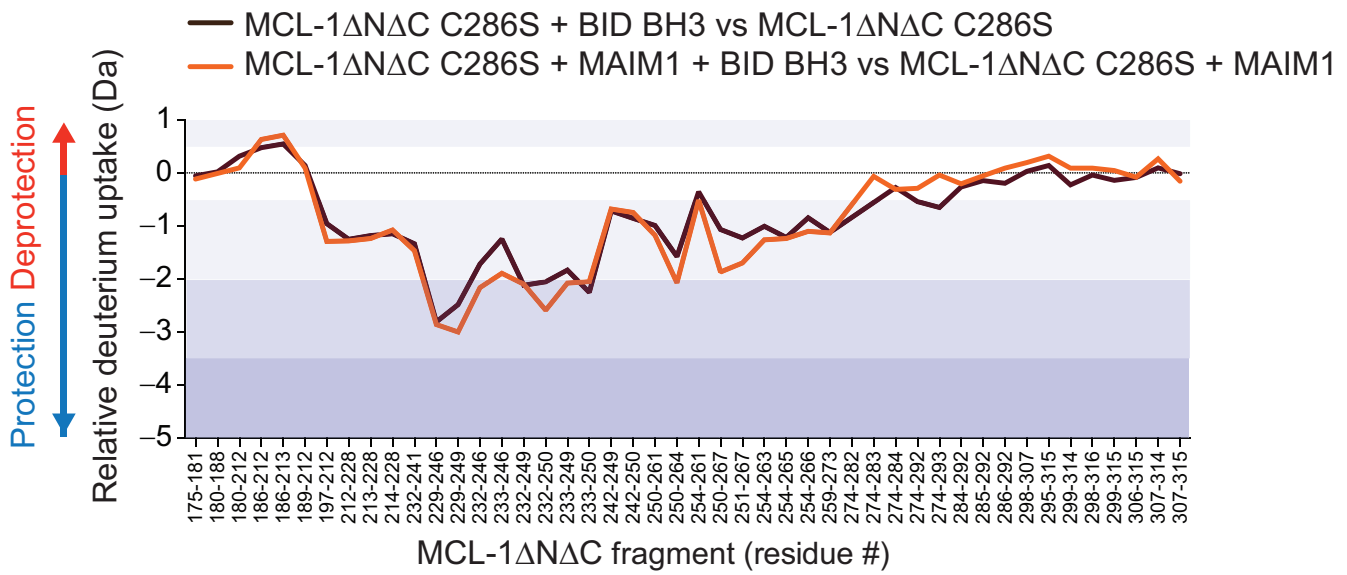

Supplementary Figure 2

C286S mutagenesis abrogates the MAIM1 effect on deuterium exchange of MCL-1ΔNΔC in the presence of BID BH3

Relative difference plots of the relative deuterium incorporation of MCL-1ΔNΔC C286S in the presence of BID BH3 minus the relative deuterium incorporation of MCL-1ΔNΔC C286S (brown), and the relative deuterium incorporation of MCL-1ΔNΔC C286S in the presence of MAIM1 and BID BH3 minus the relative deuterium incorporation of MCL-1ΔNΔC C286S in the presence of MAIM1 (orange). Changes in deuterium exchange above a stringent significant threshold of 0.8 Da are shaded light purple (0.8 – 2 Da), purple (2 – 3.5 Da), and dark purple (> 3.5 Da). HXMS data are for deuterium labeling at 10 seconds and represent the average of at least two independent experiments using distinct preparations of protein, protein conjugates, and peptide and protein mixtures.

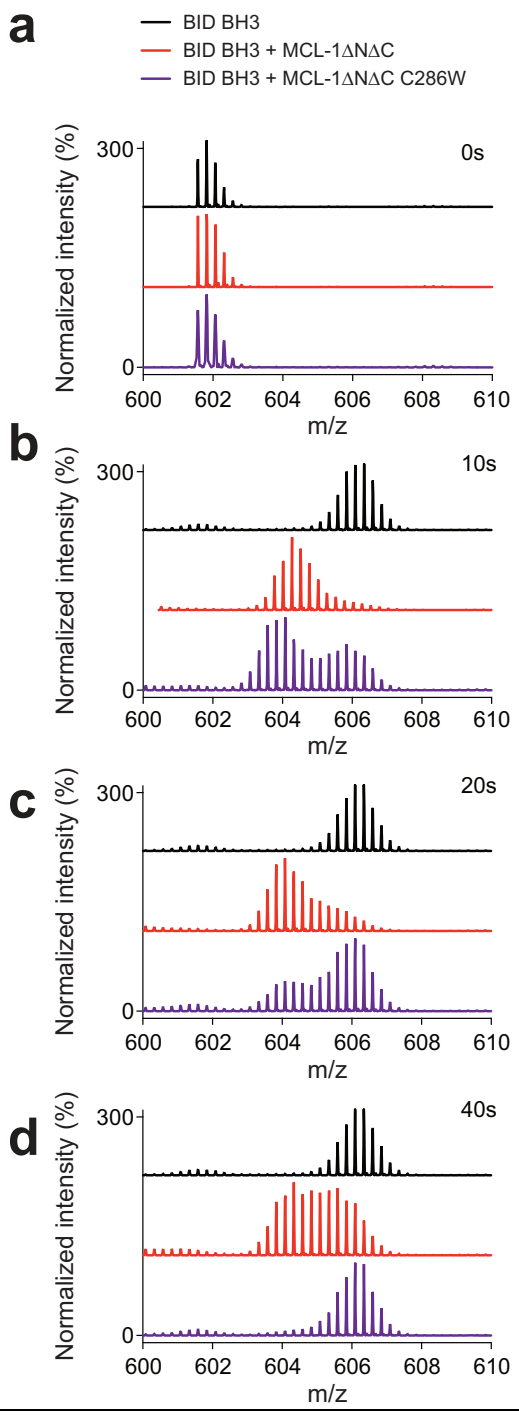

Supplementary Figure 3

C286W mutation impairs MCL-1ΔNΔC protection of BID BH3 from deuterium exchange

(**a-d**) MS spectra of BID BH3 peptide at (**a**) 0, (**b**) 10, (**c**) 20, and (**d**) 40 seconds for peptide alone (black) or the peptide combined with MCL-1ΔNΔC (red) or MCL-1ΔNΔC C286W (purple).

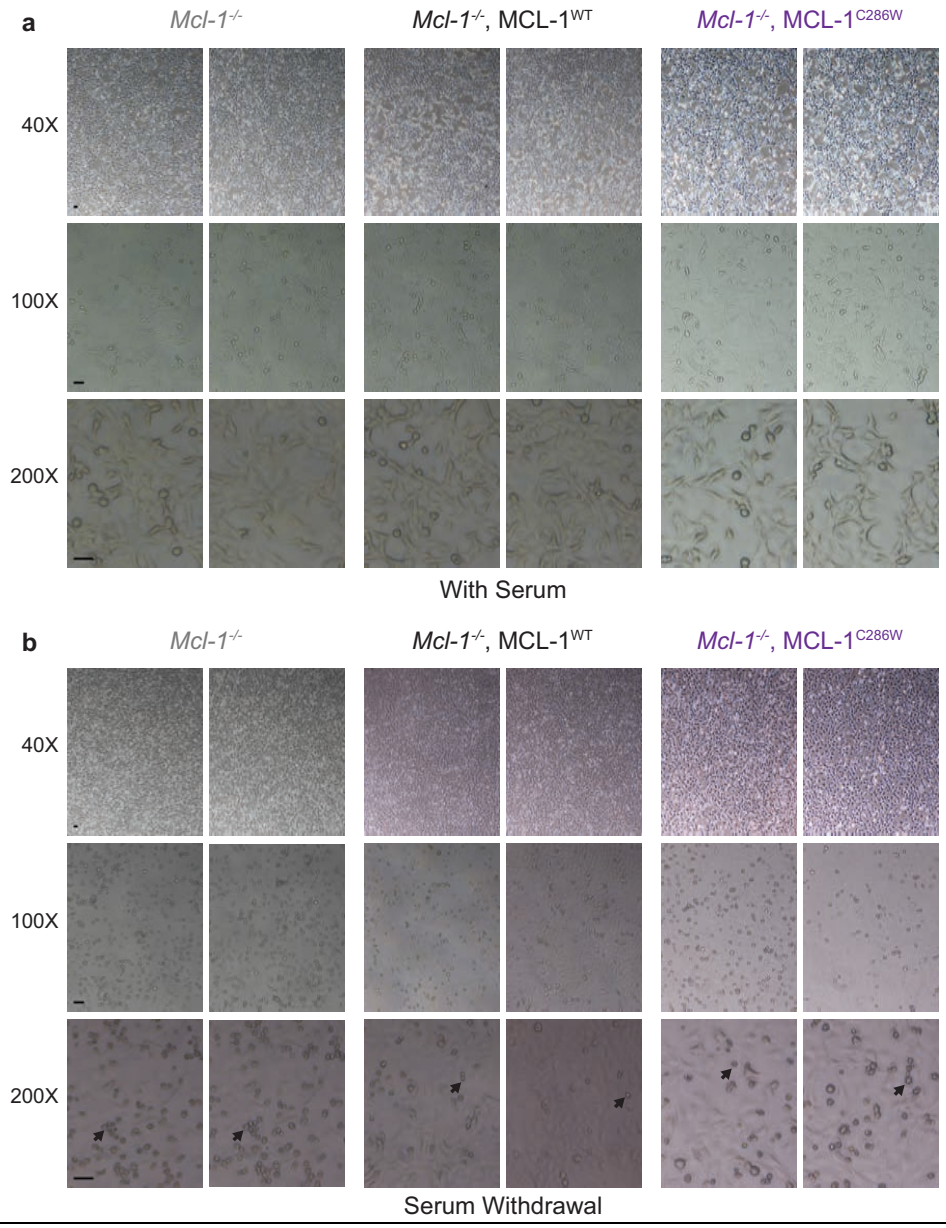

Supplementary Figure 4

Microscopic images of MEFs subjected to serum withdrawal

The indicated MEFs were maintained in **(a)** full media or **(b)** serum-free media for 16 h, followed by phase contrast microscopic imaging. Exemplary apoptotic bodies are indicated by the black arrows. Bar, 25 μm.

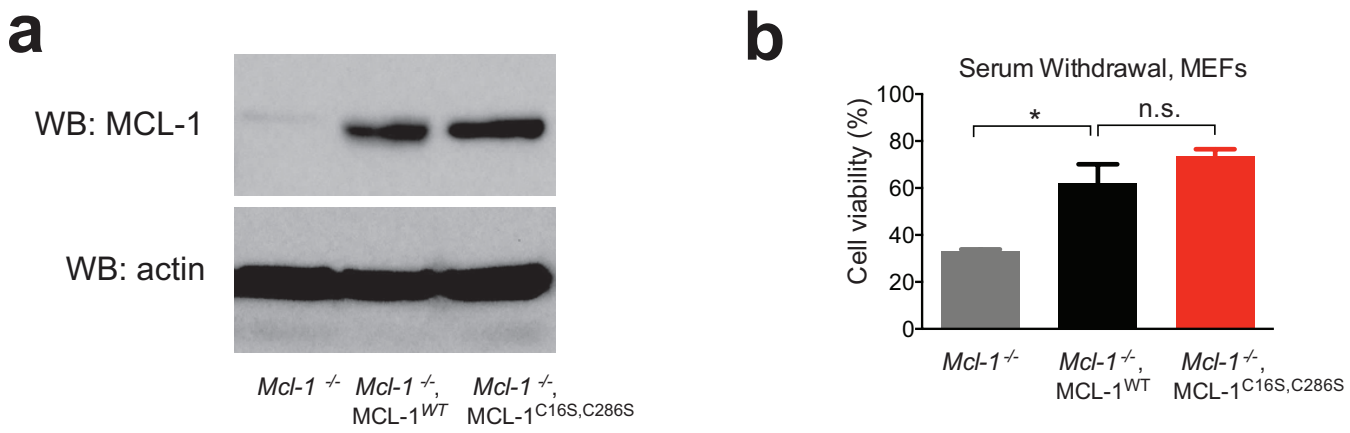

Supplementary Figure 5

C286S mutagenesis does not affect the cell viability response to serum withdrawal of MCL-1-reconstituted MEFs

(a) Western blot of lysates from *Mcl-1*$^{-/-}$ MEFs reconstituted with comparable levels of human, full-length, wild-type or C16S,C286S mutant MCL-1. **See also Supplementary Data Set 1**. **(b)** Cell viability (48 h) for the indicated MEFs subjected to serum withdrawal. Data are normalized to the corresponding MEFs maintained in complete media. Error bars are mean ± s.d. (*n* = 3 technical replicates). *, p <0.01 by two-tailed student's t test; n.s., not statistically significant.

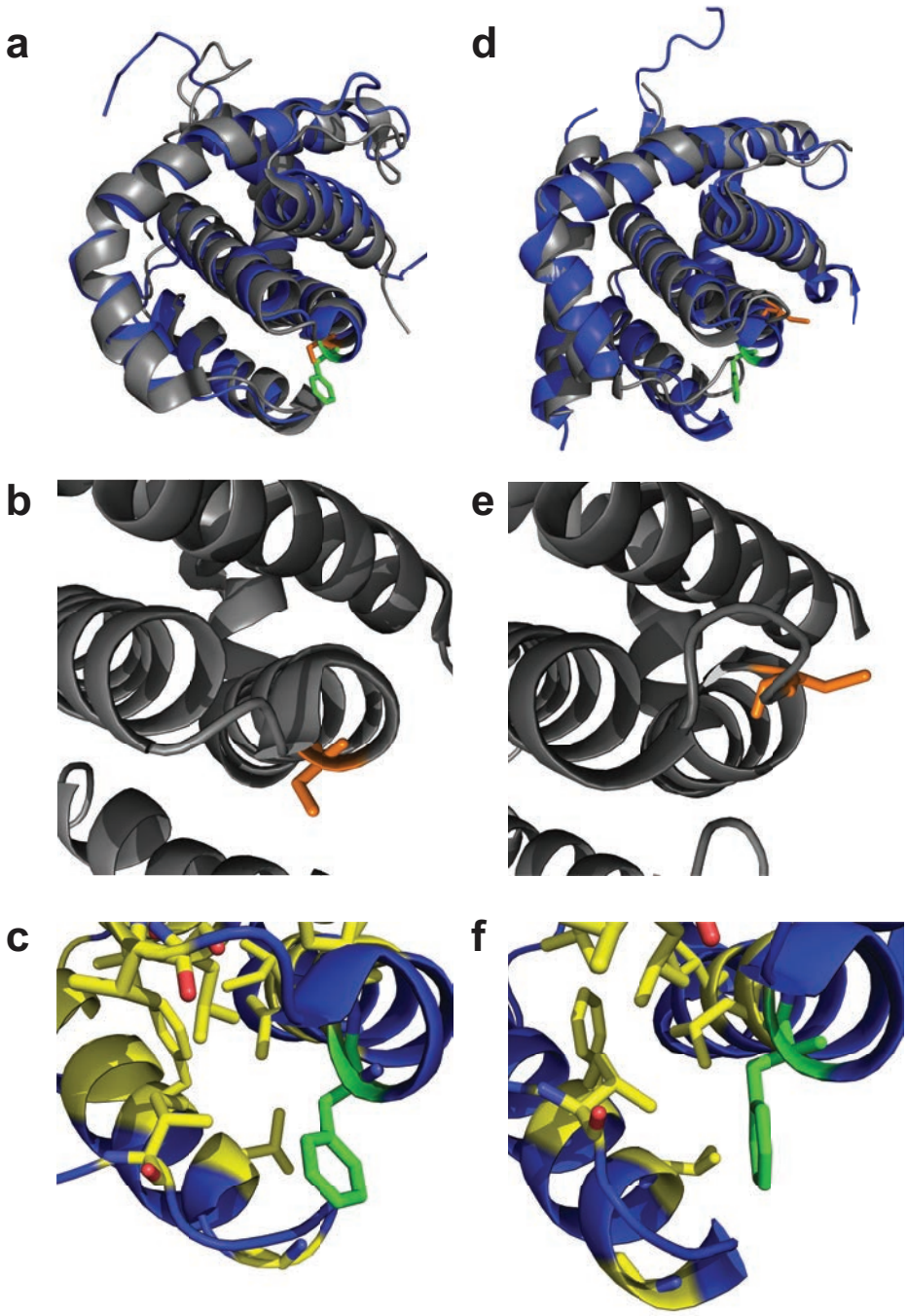

Supplementary Figure 6

Comparison of human and murine structures of MCL-1 in the C286/F267 region

(**a-c**) An overlay of the unliganded human (grey, PDB ID 2MHS) and murine (blue, PDB ID 1WSX) forms of MCL-1 demonstrate a similar structural disposition of C286 and F267 (**a**), with C286 (orange) pointing toward the surface (**b**) and F267 (green) juxtaposed to a confluence of internal hydrophobic residues (yellow) (**c**). (**d-f**) In contrast, an overlay of BH3-liganded forms of human (grey, PDB ID 2PQK) and murine (blue, PDB ID 2ROC) MCL-1 demonstrate differential orientations of C286 and F267 (**d**), with the location of C286 (orange) shifted within a relatively more unfolded region of the protein but still pointing toward the surface (**e**), and F267 (green) slightly torqued but with similar orientation and adjacency to internal hydrophobic residues (yellow) (**f**).

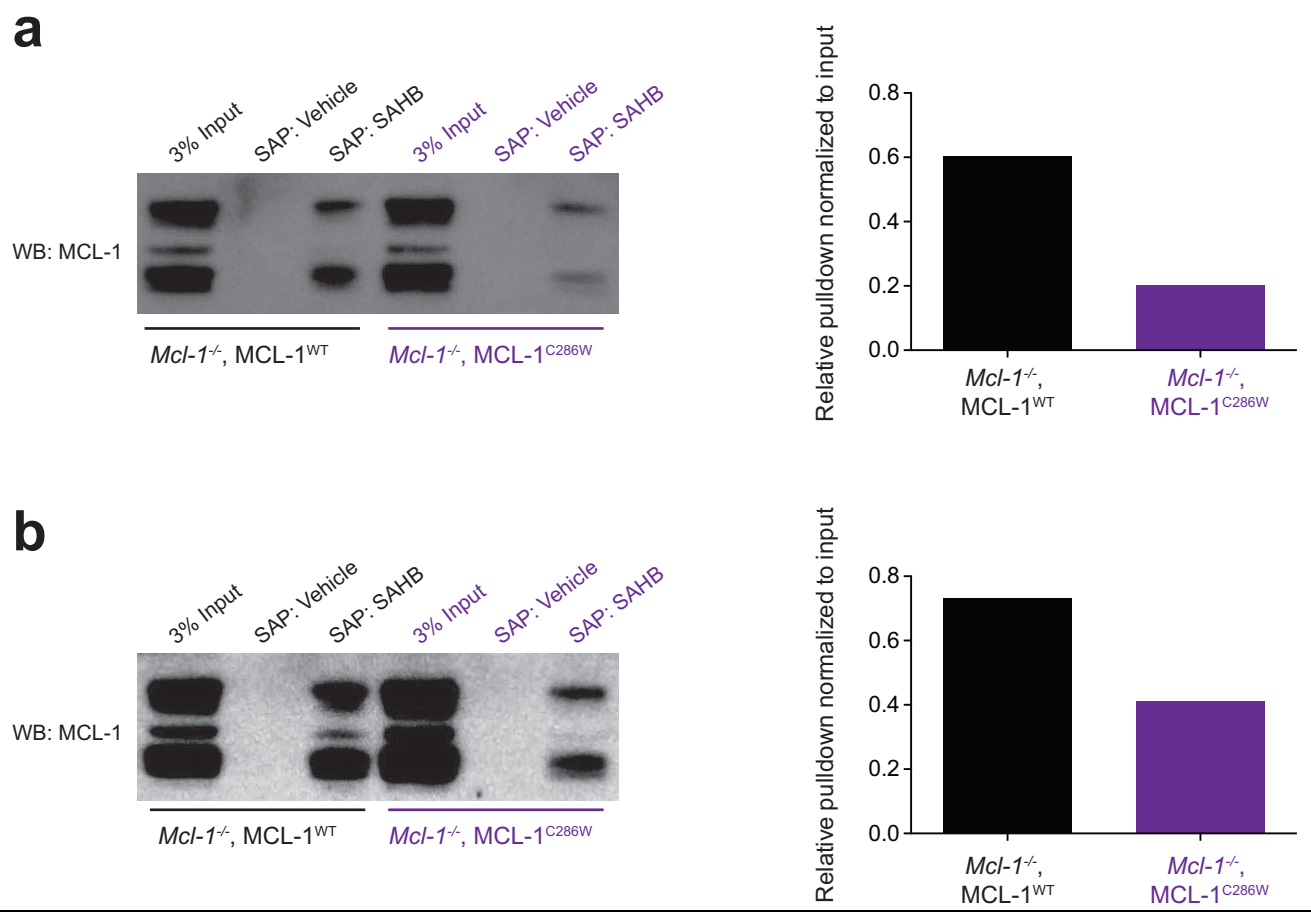

Supplementary Figure 7

Comparative BH3-based pull down of MCL-1 and MCL-1 C286W from reconstituted *Mcl-1*$^{-/-}$ MEFs

(a-b) Western blots of streptavidin pull-downs from lysates of the indicated MEFs treated with biotinylated MCL-1 $SAHB_D$, a selective stapled BH3 inhibitor of MCL-1 (left). See also **Supplementary Data Set 1.** The relative amount of precipitated MCL-1 vs. MCL-1 C286W was quantitated by densitometry of immunoreactive MCL-1 bands in the pull-down as ratioed to input control (right). Two independent streptavidin pull-down (SAP) experiments from treated lysates of the MEF cultures are shown.